

# Lawrence Berkeley National Laboratory

## Lawrence Berkeley National Laboratory

### Title

Modeling Hydraulic Responses to Meteorological Forcing: from Canopy to Aquifer

### Permalink

<https://escholarship.org/uc/item/6vk0j97w>

### Authors

Pan, Lehua  
Jin, Jiming  
Miller, Norman  
et al.

### Publication Date

2008-06-20

Peer reviewed

2                   **Modeling Hydraulic Responses to Meteorological Forcing:**  
3                                   **From Canopy to Aquifer**

4  
5           Lehua Pan, Jiming Jin, Norman Miller, Yu-Shu Wu, and Gudmundur Bodvarsson

6  
7                   Earth Sciences Division, Lawrence Berkeley National Laboratory  
8                                   MS 90-1116  
9                                   One Cyclotron Road, Berkeley, CA 94720

10  
11  
12  
13  
14  
15  
16  
17  
18  
19  
20  
21  
22  
23  
24  
25  
26  
27  
28                                   lpan@lbl.gov  
29



2 the land surface as the upper boundary, by lumping the complex processes above the  
3 surface as known boundary conditions (e.g., net infiltration or hydraulic head). However,  
4 in nature, the hydraulic processes from canopy to aquifer often form an integrated  
5 surface-subsurface system through complicated interactions. As a result, such simplified  
6 models cannot properly describe how the real system behaves, in many cases resulting in  
7 unacceptable errors. During the last few decades, much progress has been made in  
8 developing of more realistic models to simulate hydraulic interactions through the land  
9 surface. Instead of simply taking the land surface as the boundary of the modeling  
10 domain, many recent models simulate the lower portion of the atmosphere and upper  
11 portion of the subsurface as an integrated system with various approaches, by which the  
12 atmosphere-land interactions become internal processes (Abromopoulos et al., 1988;  
13 Famiglietti and Wood, 1991; Wood et al., 1992; Liang et al., 1994; Bonan, 1998; Dai and  
14 Zheng, 1997; Walko et al., 2000; Gutowski et al., 2002; York et al., 2002; Liang et al.,  
15 2003; Olesen et al., 2004; Niu and Yang, 2006). CLM3 is one such model primarily  
16 developed to meet the needs of regional climate modeling. In CLM3, radiation, sensible  
17 and latent heat transfer, zonal and meridional surface stresses, and ecological and  
18 hydrological processes are simulated as interrelated subprocesses, using hybrid  
19 approaches (i.e., combinations of physically based dynamic modeling and experientially  
20 based parameterization models). However, the model of subsurface moisture flow in  
21 CLM3 is still overly simplified. In this regard, TOUGH2 can offer a more realistic  
22 physical process-based modeling capability for subsurface hydrologic processes  
23 (including heterogeneity, three-dimensional flow, seamless combining unsaturated and  
24 saturated zones, and water table). Therefore, coupling these two models is an attractive  
25 way to build a useful model of surface-subsurface hydraulic system.

26  
27 The objectives of this study are (1) to develop a new model of atmosphere-land-  
28 subsurface hydraulic interactions at watershed or regional scales by combining the best  
29 aspects of both CLM3 and TOUGH2; (2) to show the importance of realistically  
30 modeling both surface and subsurface processes, as well as their interactions in predicting  
31 the hydrologic responses to meteorological forces, by applying the new model to a  
32 watershed in Russia over an 18-year period.

## 33 34 **2. Modeling approaches**

35 The new model, CLMT2, can be seen as combining CLM3 and TOUGH2 (Module EOS9  
36 only, called “TOUGH2” below for simplicity) in a sequential coupling. It inherits most of  
37 the modeling capabilities of both CLM3 and TOUGH2. A detailed technical description  
38 of CLM3 can be found in the NCAR Technical Note (Oleson et al., 2004), whereas Wu et  
39 al. (1996) provided a summary of EOS9, an unsaturated/saturated water flow simulation  
40 module, within the TOUGH2 package.

41  
42 From the perspective of CLM3, the new model no longer simulates the subsurface  
43 moisture movement as a one-dimensional process by explicit scheme. Instead, the 3-D  
44 Richards equation is solved implicitly by TOUGH2. In particular, the assumption that the  
45 permeability decreases exponentially from top to bottom of the soil is no longer used, and  
46 the groundwater depth is no longer a parameter calculated as saturation-weighted depth.  
47 Therefore, CLMT2 can be more flexible in dealing with complex subsurface

2 environments. From the perspective of TOUGH2, the new model no longer takes the net  
 3 infiltration or root uptake as a prescribed boundary condition or source/sink term. Instead,  
 4 the net infiltration and root uptake result from simulations of coupled energy, wind,  
 5 vegetation, and hydraulic processes by CLM3. As a result, CLMT2 expands the scope of  
 6 TOUGH2 such that more realistic modeling of land-surface conditions is possible.

7  
 8 Table 1 lists the major differences in simulating subsurface flow between CLM3 and the  
 9 coupled model, CLMT2.

10  
 11 Table 1 Major differences between CLM3 and CLMT2 in simulation of subsurface flow

CLM3	CLMT2
Assumes that permeability decreases with depth exponentially.	Spatially variable permeability is user specified
Richards equation is solved explicitly (no iteration in each time step).	Richards equation is solved fully implicitly.
Clapp and Hornberger relationships are used for hydraulic functions of soil.	Van Genuchten relationships are used for hydraulic functions of soil.
Hydraulic properties are assigned generally based on the soil texture classification.	Hydraulic properties are provided as input by the user for the specific site.
Soil moisture stress for root uptake is either 0 or 1 (dead or live).	A piecewise linear function is used to simulate the soil moisture stress for root uptake.
Soil columns are isolated from one another and subsurface drainage (base flow) is calculated as a value proportional to the saturation weighted average $K_s$ in lower soil layers and $\exp(-WT)$ , which is then deducted from the soil each time step.	Lateral subsurface flow if any is included naturally in three-dimensional flow simulation. No artificial subsurface drainage is included.
Soil depth is limited to 3.5 meters.	Soil depth, usually larger than 3.5 meters, is specified by the user so that the domain bottom is deeper than the water table.

12  
 13  
 14  
 15 **2.1 Spatial discretization and grid structure of CLMT2**

16 The modeling domain below land surface is discretized into connected grid cells  
 17 similar to a TOUGH2 grid. Different from a regular TOUGH2 grid, however, the grid  
 18 cells in the upper portion (the root zone) of a CLMT2 grid must be geometrically  
 19 “regular”, so that they can form grid columns. The aerial extent of each grid column  
 20 corresponds to the grid cell of a regional climate model. Above each grid column,  
 21 nested hierarchical grid structures are created to capture land-surface heterogeneity  
 22 within the area. An area can contain multiple, noninteractive landunits (e.g., “glacier”,  
 23 “wetland”, “vegetated”, “lake”, and/or “urban”). Each landunit (except “lake”) can

2 contain multiple, noninteractive “snow/soil” sub-columns. Similarly, each  
 3 “snow/soil” type can contain multiple, noninteractive plant functional type (PFT)  
 4 patches (Bonan et al., 2002). The term “noninteractive” indicates that there is no  
 5 communication among substructures at the same level. In other words, they are  
 6 logically isolated subareas splitting the entire area. Besides the “snow/soil”  
 7 subcolumns, which can have multiple layers, all other substructures are one-layer or  
 8 single-node structures. Note that the “soil” subcolumns spatially overlap the root zone  
 9 of the subsurface grid column where the communication between TOUGH2 and  
 10 CLM3 takes place. In addition, the “snow/soil” subcolumns are also used for  
 11 calculations of thermal transfer and freezing/melting processes in snow cover and soil,  
 12 because EOS9 of TOUGH2 does not account for those processes.

## 14 2.2 Modeling of processes in CLMT2

15  
 16 Models of water flow in subsurface is based on numerical solutions of the Richards  
 17 equation:

$$19 \frac{\partial \theta}{\partial t} = \nabla \cdot [k_s k_r \nabla \psi_h] + q_s - q_{root} \quad (1)$$

20  
 21 with a flux continuation condition at land surface:

$$23 -k_s k_r \left. \frac{\partial \psi_h}{\partial z} \right|_{at \text{ landsurface}} = q_{net} \quad (2)$$

24  
 25 where  $\theta$ ,  $\psi_h$ ,  $k_s$ ,  $k_r$  are the volumetric water content, the hydraulic potential, the  
 26 saturated hydraulic conductivity, and the relative permeability, respectively. The term  
 27  $q_{root}$  is root uptake rate while  $q_s$  indicates other source/sink terms that might exist in  
 28 the subsurface (e.g., wells). The root uptake rate varies spatially and depends on the  
 29 root distribution in the root zone and the transpiration from dry leaf surfaces ( $E_v^t$ ):

$$31 q_{root} = E_v^t r(z) = \left[ -\frac{\rho_{atm} (h_{can} - h_{can}^{sat})}{r_b} r_{dry} \beta_t \right] r(z) \quad (3)$$

32  
 33 where  $r(z)$ , varying with the depth  $z$ , is the effective root fraction, a product of the  
 34 root fraction and the soil stress. The terms  $\rho_{atm}$ ,  $h_{can}$ ,  $h_{can}^{sat}$ ,  $r_b$ , and  $\beta_t$  are the density  
 35 of atmospheric air, the specific humidity of canopy air, the saturated water-vapor  
 36 specific humidity at the vegetation temperature, the leaf boundary stomatal resistance,  
 37 and the total soil moisture stress to the root uptake, respectively. The shade factor  
 38 ( $r_{dry}$ ) is calculated as a function of the sunlit ( $L^{sun}$ ) and shaded ( $L^{sha}$ ) leaf area  
 39 indices:

$$r_{dry} = \frac{f_{dry} r_b}{L} \left[ \frac{L^{sun}}{r_b + r_s^{sun}} + \frac{L^{sha}}{r_b + r_s^{sha}} \right] \quad (4)$$

The term  $f_{dry}$  is the fraction of leaves that are dry,  $L^{sun}$  and  $L^{sha}$  are the sunlit and shaded leaf area indices, and  $r_s^{sun}$  and  $r_s^{sha}$  are the sunlit and shaded stomatal resistances, respectively.

The net infiltration rate ( $q_{net}$ ) in Equation (2) is calculated from the surface water-balance equation (the run-on process is not simulated in the model and all runoff water will be removed immediately):

$$q_{net} = q_0^{liq} - q_{runoff} - E_g \quad (5)$$

where  $q_0^{liq}$  is the rate of liquid water reaching the soil surface. It could be the summation of throughfall rate ( $q_{thru}^{liq}$ ) and canopy drip rate ( $q_{drip}^{liq}$ ) if no snow cover exists or the flow rate of liquid water reaching the soil surface from the snow layers (including melting water). The throughfall rate is the liquid precipitation ( $q_{rain}$ ) that directly falls through the canopy and is calculated as:

$$q_{thru}^{liq} = q_{rain} \exp[-0.5(L+S)] \quad (6)$$

where  $L$  and  $S$  are the exposed leaf and stem area index, respectively. The canopy drip rate is calculated from the canopy interception model, while the flow rate of liquid water reaching soil surface from the snow layers is an output of the snow processes model. Both models are described in detail in the NCAR Technical Note (Oleson et al., 2004) and will not be repeated here.

The other two terms in Equation (5), the surface runoff ( $q_{runoff}$ ) and the water vapor flux at soil surface ( $E_g$ ), along with the transpiration ( $E_v^t$ ) and the net infiltration rate ( $q_{net}$ ) mentioned above, are four important fluxes that connect the surface and subsurface processes in CLM2.

If the top soil layer is not impermeable, the surface runoff is the sum of runoff from saturated and unsaturated areas:

$$q_{runoff} = [f_{sat} + (1 - f_{sat})w_m^4] q_0^{liq} \quad (7)$$

where  $f_{sat}$  and  $w_m$  are the fraction of saturated area and the mean wetness in the top three layers, respectively. In particular, the fraction of saturated area is a function of water table depth ( $z_w$ ):

$$f_{sat} = w_{fact} \min[1, \exp(-f_z z_w)] \quad (8)$$

where  $w_{fact}$  and  $f_z$  are the fraction of wet land area and a constant scaling factor ( $f_z = 1 \text{ m}^{-1}$ ), respectively.

The water vapor flux at soil surface ( $E_g$ ) reflects the net result of soil surface evaporation and dew. It is driven by the gradient of specific humidity between the ground surface and the atmosphere (nonvegetated surface) or the canopy (vegetated surface) as follows:

$$E_g = -\frac{\rho_{atm} (h_{atm} - h_g)}{r_{aw}} \quad (9a)$$

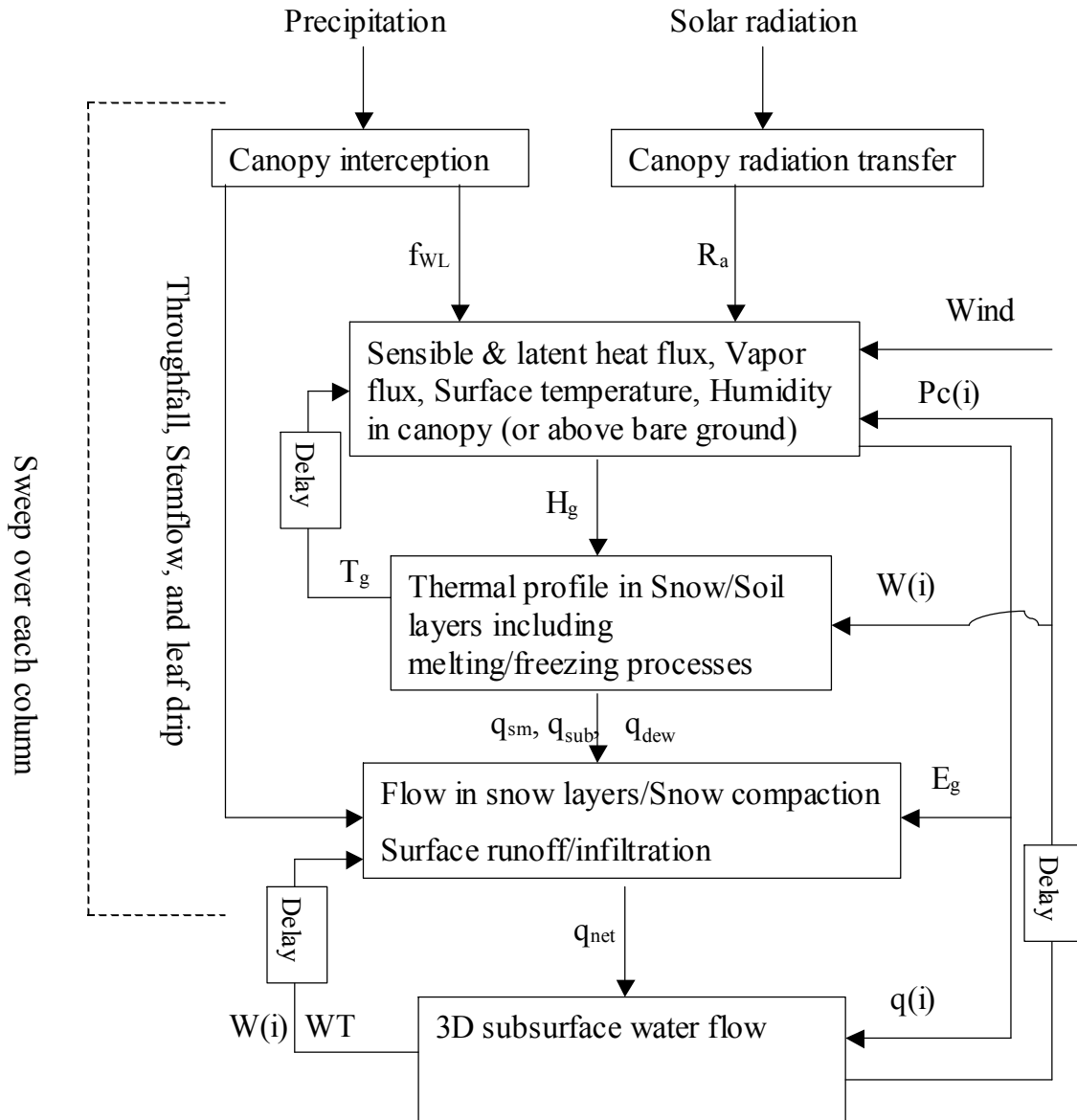
for nonvegetated surface, and

$$E_g = -\frac{\rho_{atm} (h_{can} - h_g)}{r_{agc}} \quad (9b)$$

for a vegetated surface, where  $\rho_{atm}$ ,  $h_{atm}$ ,  $h_g$ , and  $h_{can}$  are the density of atmospheric air, the atmospheric specific humidity, the specific humidity of the soil surface, and the canopy air specific humidity, respectively. The other two terms,  $r_{aw}$  and  $r_{agc}$ , are the aerodynamic resistance to water vapor transfer between the ground and the atmospheric air at the reference height, and that between the ground and the canopy air, respectively. The aerodynamic resistances are calculated using a surface-layer model based on Monin-Obukhov similarity theory. The water-vapor flux is simulated as a part of the coupled surface energy, momentum, and moisture model, described in detail in the NCAR Technical Note (Oleson et al., 2004) and not repeated here.

Figure 1 shows a brief flow chart of CLMT2 for one time step. For a given meteorological forcing at each time step, CLM3 modules simulate canopy and surface processes sequentially and column by column, using the water table (WT), water content (W(i)), and capillary pressure (Pc(i)) calculated by the TOUGH2 module at the previous time step. The resulting net infiltration rate ( $q_{net}$ ) and root uptake flux ( $q(i)$ ) are then used as source/sink terms in subsurface flow simulation by the TOUGH2 module. This sequential coupling approach is mass conserved but could be inaccurate if the size of time step was too large. However, the time step required for simulating the surface processes by CLM3 is usually so small (e.g., in order of hours) with respect to the subsurface processes that the sequential coupling approach shall not add any new time-stepping limit.





$f_{WL}$ —fraction of wet leaf;  $R_a$ —absorbed radiation flux;  $T_g, H_g$ —ground temperature and heat flux;  $q_{sm}, q_{sub}, q_{dew}$ —water flux of snow melting, sublimation, and dew;  $E_g$ —evaporation at ground;  $q(i), W(i), Pc(i)$ —root uptake flux, water content, and capillary pressure in root zone;  $WT$ —groundwater table;  $q_{net}$ —net infiltration

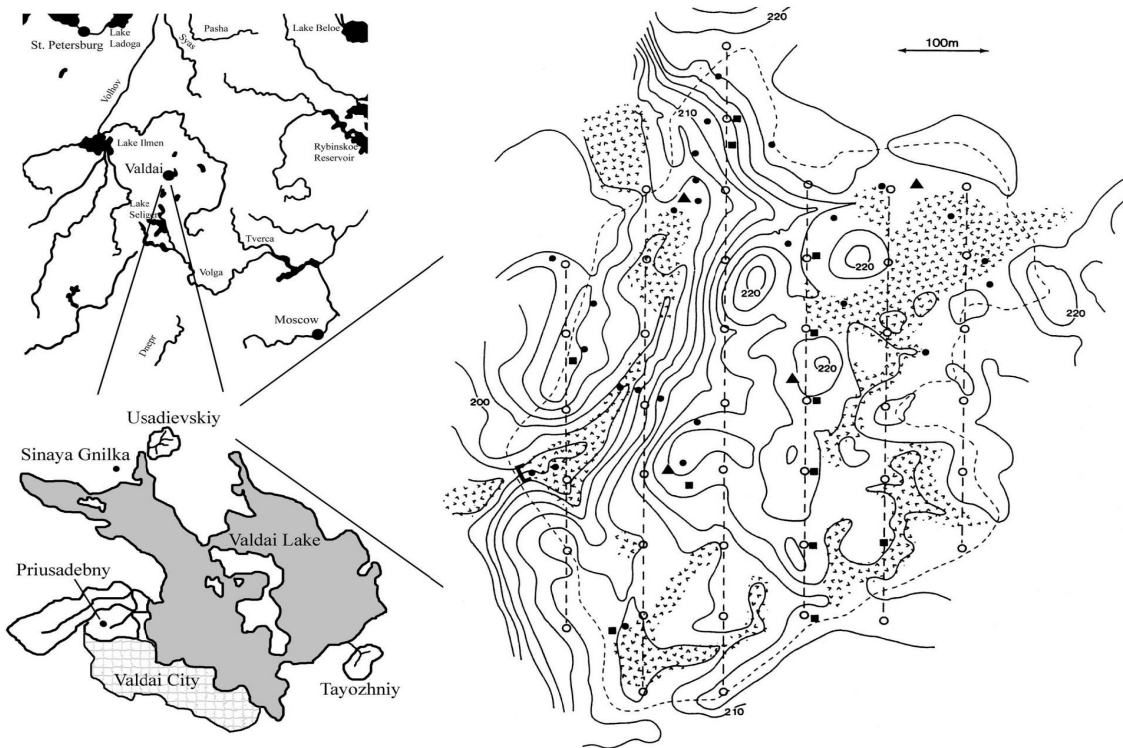
2  
3  
4  
5

Figure 1 Flow chart of CLMT2 (“Delay” indicates the values in the previous time step are used.)

2  
3  
4  
5  
6  
7  
8  
9  
10  
11

### 3. Results and Discussion

Usadievsky Catchment, Valdai, Russia, is a midlatitude grassland catchment, with deep snow cover in the winter and significant precipitation in the summer. Eighteen years of observation data related to this catchment were used extensively within the Project for Intercomparison of Land-surface Parameterization Scheme (PILPS) and provided a very robust validation for surface-subsurface models (Maxwell and Miller, 2005). All of the observations were made available by Robock et al. (2000) and Luo et al. (2003) as part of the Global Soil Moisture Databank. The precipitation data within the original



**Figure 2. Map of the Usadievskiy catchment at Valdai, Russia and its location (adapted from Fig. 1 in Luo et al., 2003). Filled circles are water-table measurement sites. Open circles with dashed lines indicated the snow measurement sites and routes, respectively. Discharge is measured at the stream outflow point of the catchment (see bold bracket) at the lower left-hand corner of the catchment map. Filled triangles indicate the measurement sites of soil freezing and thawing depths. The short dash line denotes the catchment boundary. Hatched areas denote regions of swampy conditions. Elevation contours are in increments of 2 m.**

12  
13  
14  
15  
16  
17  
18

meteorological forcing data at 3 hr intervals were scaled by the observed monthly precipitation, so that the precipitation as model input was consistent with the observed ones at the temporal scale of one month.

For subsurface simulation in CLM2, the hydraulic parameters used in this study are the same as those in Maxwell and Miller (2005). The entire catchment (0.36 km<sup>2</sup>) is simulated as a 1-D column down to the depth of 6 m. The vertical discretization of

2 subsurface is 0.1 m except the top two cells for which 0.01 m and 0.09 m are used,  
 3 respectively. Table 2 lists the major model parameters used in the simulation.

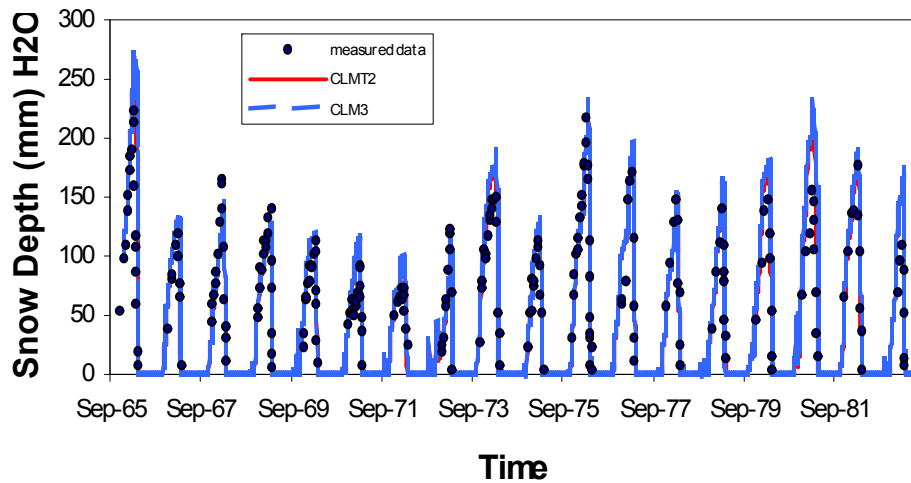
4  
 5 Table 2. Model parameters used in Vaidai simulation

Parameter	Value	Unit
Van Genuchten alpha	1.95	m <sup>-1</sup>
Van Genuchten exponent	1.74	Unitless
Saturated hydraulic conductivity	1.21	m/day
Effective soil porosity	0.401	m <sup>3</sup> /m <sup>3</sup>
Residual saturation	0.136	Unitless
Lower critical point at which root uptake stops	-5270.81	mm H2O
Upper critical point at which root uptake stops	0.1	mm H2O
Fraction of model area with high WT	0.15	Unitless
Latitude	57.6N	Degree
Longitude	33.1E	Degree
Vegetation type index	7 (grassland)	Unitless
Soil type index	6 (loam)	Unitless

6  
 7 For subsurface simulation in CLM3, The entire catchment (0.36 km<sup>2</sup>) is also simulated as  
 8 a 1-D column but the depth of the domain is 3.5 m as hard coded in CLM3. Furthermore,  
 9 the vertical spatial discretization varies from 0.0175 m to 1.137 m from top to bottom,  
 10 which is also hard-coded in CLM3.

11  
 12 All the parameters for the land surface and the meteorological forcing data are the same  
 13 for both models.

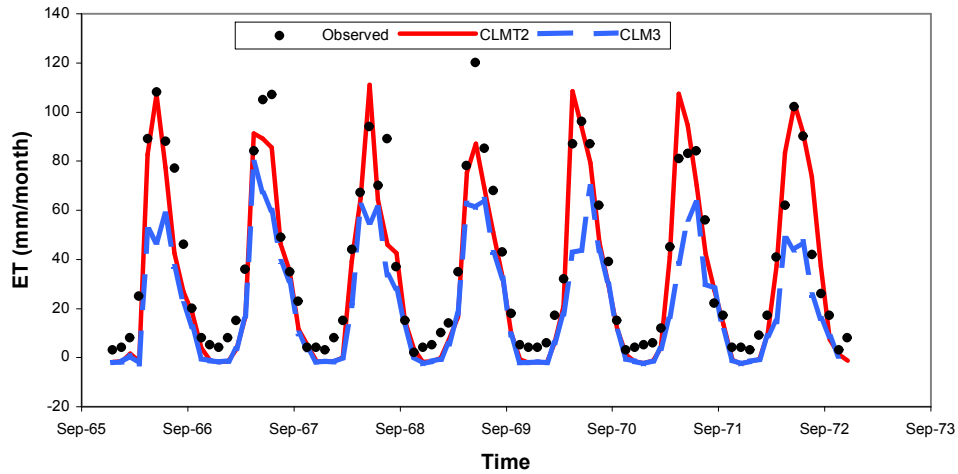
14  
 15 The simulated and observed daily snow depths are presented in Figure 3. Both CLM3  
 16 (blue dash line) and CLMT2 (red solid line) predict almost identical results that agree  
 17 well with the observed snow depth (the dots). This convergence between the two models



18  
 19 Figure 3. Simulated and observed snow depth (in mm of equivalent water)

2 is expected, because of the halt in surface-subsurface hydraulic interactions during the  
3 frozen winter season. As a result, the accuracy of the subsurface simulation does not  
4 matter in simulating the snow accumulation process on the land surface.

5 However, CLMT2 does significantly improve the predictions of monthly  
6 evapotranspiration (ET) (Figure 4). As shown in Figure 4, CLM3 underestimated the ET  
7 compared with the observed data, whereas CLMT2 is in close agreement with the  
8 observed data. This model improvement can be evaluated quantitatively by the model  
9 efficiency (E) proposed by Nash and Sutcliffe (1970) that is defined as one minus the  
10 sum of the squared differences between the predicted and observed values normalized by  
11 the variance of the observed values during the period under investigation. The range of E  
12 lies between 1.0 (perfect predict) and  $-\infty$ . For the 84 months of monthly ET data shown in  
13 Figure 4, E is 0.635 for CLM3 and 0.865 for CLMT2, respectively. The improvement is  
14 significant.



15

16

**Figure 4 Simulated and observed monthly ET**

17

18

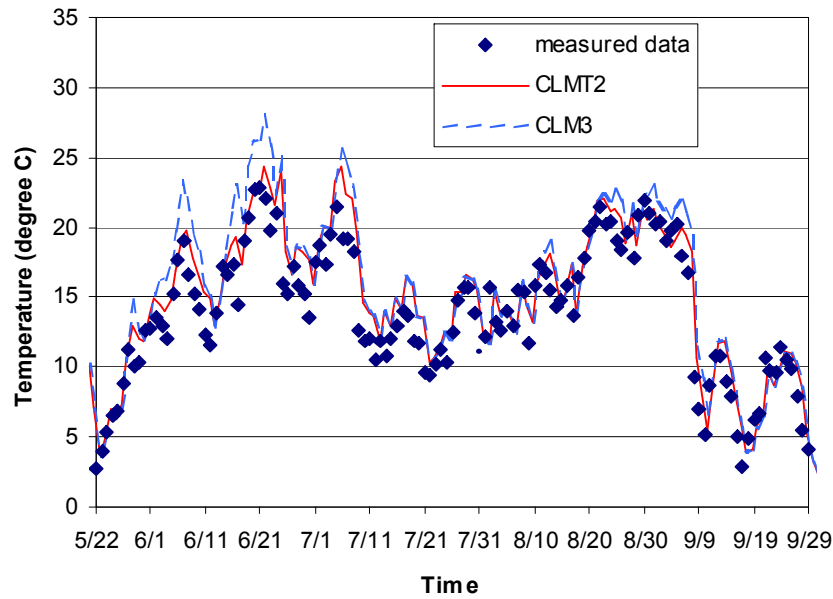
19

20

21

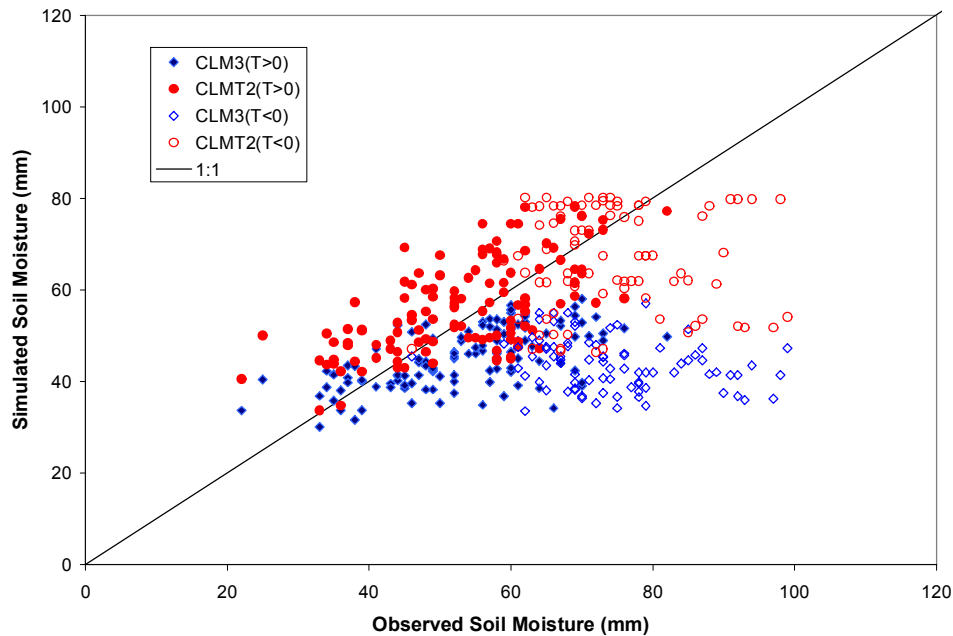
22

Consistent with underestimating ET, CLM3 often overestimates the surface temperature during the summer season (Figure 5, only 6-9 months of 1968 shown for a clear presentation, others are similar). Obviously, the coupled model, CLMT2, is more accurate in this case as well. These results indicate that the impact of subsurface flow on surface processes during nonfrozen seasons is significant, and that correctly simulating the subsurface flow is very important.



2  
3 **Figure 5. Simulated and observed ground surface temperature during summer (05/22/1968-**  
4 **09/29/1968 shown, others are similar)**

5 ET is one of the important moisture and energy exchanges between land and atmosphere,  
6 and is the most unique process that tightly connects the near-surface atmosphere,  
7 vegetation, soil, and groundwater together. The temperature, humidity, and wind speed  
8 are three major meteorological factors that drive ET processes. The canopy structure and  
9 wetness regulate how effective these factors will be in driving the ET processes, whereas  
10 the type of plant root controls how deeply the subsurface moisture movement will be  
11 affected. Meanwhile, soil moisture status in the root zone directly controls the availability  
12 of the soil moisture for ET, while the groundwater serves as a major buffer that tends to  
13 reduce soil moisture variations. Logically, the major reason for CLM3 to underestimate  
14 the ET would be its underestimation of the soil wetness in the root zone, because the  
15 modeling approaches for the surface processes are identical in the two models.  
16 Comparisons between observed moisture amounts in the top 20 cm of soil and the values  
17 predicted by CLM3 and CLMT2 confirm that this is the case (Figure 6). The observed  
18 moisture data were computed by using data from 9 to 11 observational points distributed  
19 over the basin area. Note that the observed soil moisture data contain significant noise,  
20 especially in winter when the soil is frozen, the measured moisture often exceeds the  
21 holding capacity of 802 mm for the 20 cm soil (as defined by the porosity of 0.401).  
22 Except for these outliers, the values predicted by CLMT2 are much closer to the 1:1 line  
23 than those by CLM3. The underestimation of the available soil moisture in the root zone,  
24 especially in the top 20 cm, where most roots are located, causes CLM3 to underestimate  
25 ET. Correct simulation of subsurface processes is thus important, not only in catching the  
26 dynamic responses in the subsurface itself, but also in estimating surface moisture and  
27 energy fluxes.

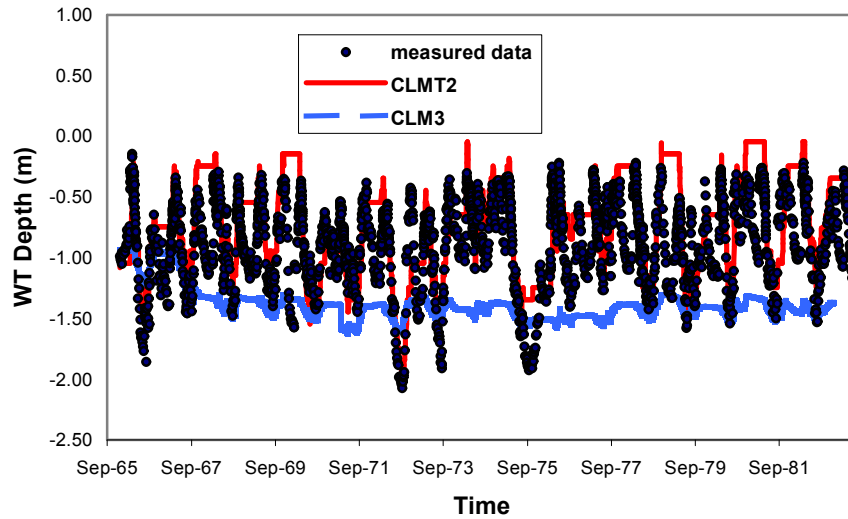


2  
3

**Figure 6. Comparison between the simulated monthly averaged moisture in the top 20 cm of soil by CLM3 (blue diamond) and CLMT2 (red circle) vs. measured data over 18 years. Here T is the monthly average ground surface temperature (°C). Therefore, T<0 indicates freezing month whereas T>0 indicates warm month.**

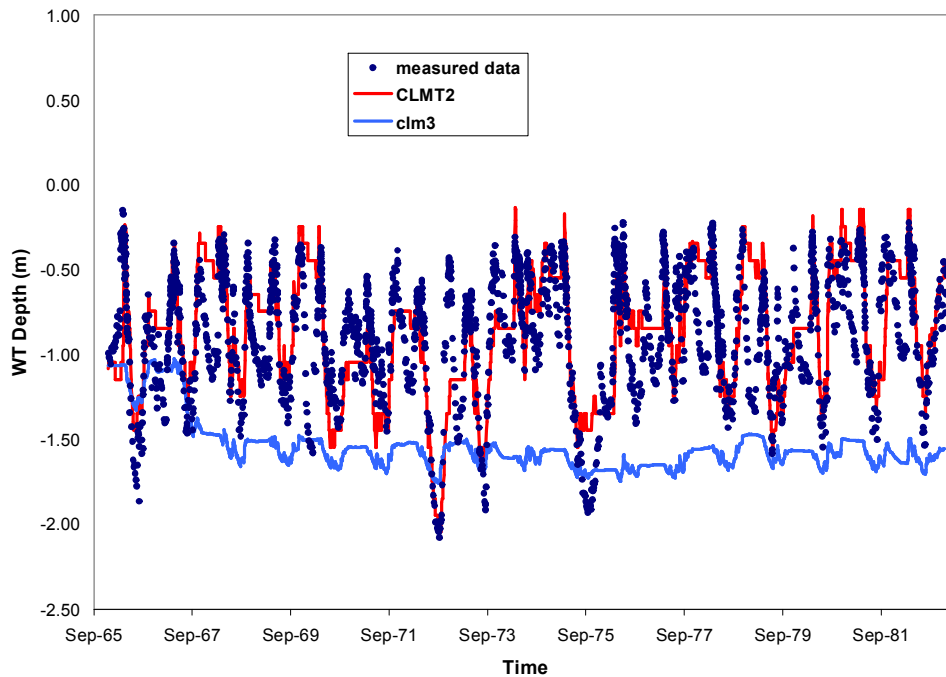
4 Furthermore, Figure 7 compares the observed daily water tables (WT) with those  
 5 simulated by CLM3 (blue line) and CLMT2 (red line), respectively. The observed WT  
 6 data are derived from a site average of 19 observation wells at a subweek scale. CLM3  
 7 uses a special parameterization scheme to calculate the WT as a soil saturation-weighted  
 8 depth, while the WT is automatically determined as the interface between the unsaturated  
 9 and saturated soil layers simulated by CLMT2. As shown in Figure 7, CLMT2 replicated  
 10 most groundwater seasonal responses to meteorological forcing. CLM3, however, poorly  
 11 estimated such responses, especially in the magnitude of WT variations. The Nash-  
 12 Sutcliffe efficiency (E) is 0.216 for CLMT2 and -3.921 for CLM3, respectively. The  
 13 negative E obtained by CLM3 indicates that the mean value of the observed time series  
 14 of water table would have been a better predictor than CLM3. Although CLM3 was not  
 15 designed to be an accurate predictor of the water table variations at first place, the result  
 16 shown in Figure 7 implies that poor estimation of water table could be an important  
 17 reason that reduces the accuracy of ET prediction. In CLM3, the assumption that the  
 18 permeability of soil decreases exponentially with the increase of the depth is used, which  
 19 unrealistically limits the moisture movement in the soil, including both unsaturated and  
 20 saturated zones. As a result, the simulated water table is much less responsive to  
 21 meteorological forcing than the reality. One of example of such weak responsiveness is  
 22 the underestimated capability of the groundwater to supply the moisture to the root zone  
 23 that feeds to the ET requirement. Furthermore, the overall low predicted water table by

2 CLM3 can be attributed to its parameterization scheme of subsurface drainage, which  
3 tends to overestimate the subsurface drainage rate.  
4



5  
6 **Figure 7. Simulated and observed daily water table (WT)**  
7

8 Note that neither models caught the lowering of the water table during winter (Figure 7).  
9 This is most likely a result of subsurface discharge flow below the frozen zone, which  
10 could not be accounted for by CLM2 with this single column model, whereas CLM3  
11 accounts for the subsurface drainage improperly, as discussed above. As a sensitivity  
12 study, a “constant-head” cell is added to the TOUGH2 grid to mimic the subsurface  
13 discharge flow in the CLM2 model. The parameters of the “constant-head” cell that  
14 regulate the subsurface discharge flow are estimated based on the stream/catchment ratio  
15 and the average slopping of the catchment. As shown in Figure 8, the water table depth  
16 simulated by CLM2 only partly catches the winter lowering of water table. The  
17 efficiency E improved to 0.439. Because the Usadievsky Catchment is a small part of the  
18 Valdai watershed (Figure 2), the subsurface discharge problem is further complicated by  
19 the unknown regional-ground water flow. Consequently, a distributed model would be  
20 required to investigate this problem (which should be a good topic for further studies).  
21 Unlike CLM3, the new model, CLM2, has the capability to simulate 3D regional  
22 groundwater flow, provided that adequate field information is available.  
23



2 Figure 8 Simulated and observed water tables (CLMT2 has a “constant head” cell)

3  
4  
5 **4. Conclusions**

6 A model that combines the ability to simulate the land-surface and subsurface hydrologic  
7 responses with meteorological forcing, CLMT2, has been developed, by combining a  
8 state-of-the-art land-surface model, the NCAR Community Land Model version 3  
9 (CLM3), and a variably saturated groundwater model, TOUGH2, through an internal  
10 interface that includes flux and state variables shared by the two submodels. CLM3  
11 provides the state-of-the-art modeling capability for surface energy and hydrologic  
12 processes, including snow, runoff, freezing/melting, evapotranspiration, radiation, and  
13 biophysiological processes. TOUGH2 offers the more realistic physical-process-based  
14 modeling capability of subsurface hydrologic processes, including heterogeneity, three-  
15 dimensional flow, seamless combining of unsaturated and saturated zone, and water table.  
16 This new model, CLMT2, preserves the best aspects of both submodels. The new model  
17 is also ready to be coupled with an atmospheric simulation model, representing one of the  
18 first models that are capable to simulate hydraulic processes from top of the atmosphere  
19 to deep-ground.

20  
21 Eighteen years of observed data from Usadievsky Watershed, Valdai, Russia, was used to  
22 evaluate the performance of the new model. Compared to the old model, CLM3, the new  
23 model, CLMT2, greatly improved the predictions of the water table, evapotranspiration,  
24 surface temperature, and the moisture in the top 20 cm of soil at the real watershed. This  
25 is particularly true in the nonfrozen season when the interactions between surface and  
26 subsurface are significant. These results also indicate that correct simulation of



2 subsurface flow (including the water table) is very important, not only in assessing  
3 subsurface water resource itself, but also in simulating surface processes such as  
4 evapotranspiration or land-surface temperature, the two most important feedback factors  
5 for regional climate. Note that, although the results obtained in this study are promising,  
6 the comparisons have been limited to a 1-D column simulation so far. Obviously, the 3-D  
7 simulation capability of CLMT2 needs to be tested in future. In particular, the modeling  
8 capability of surface lateral flow (e.g., runoff/run-on processes) needs to be improved in  
9 future development of CLMT2 in order to simulate the spatial details of the hydrological  
10 responses within a watershed. In addition, modeling the hydrologic processes in the  
11 frozen soil (i.e., non-rigid media) is another challenge for improving CLMT2, as revealed  
12 in comparison with the observed soil moisture data.

## 16 5. References

17 Abromopoulos, F., C. Rosenzweig, and B. Choudhury, 1988, Improved ground  
18 hydrology calculations for global climate models (GCMs): Soil water movement and  
19 evaporation. *J. Climate*, 1:921-941.

20 Bonan, G. B., 1998, A Land Surface Model (LSM version 1.0) for ecological,  
21 hydrological, and atmospheric studies: Technical description and user's guide. NCAR  
22 Tech. Note NCAR/TN-417\_STR.

23 Bonan, G.B., S. Levis, L. Kergoat, and K.W. Olesen, 2002, Landscapes as patches  
24 of plant functional types: An integrating concept for climate and ecosystem models.  
25 *Global Biogeochem. Cycles* 16:5.1-5.23.

26 Clapp, R. B., and G. M. Hornberger, 1978, Empirical equations for some soil  
27 hydraulic properties. *Water Resources Researches*, 14:601-604.

28 Dai, Y. J., and Q.-C. Zeng, 1997, A land surface model (IA94) for climate studies.  
29 Part I: Formulation and validation in offline experiments. *Adv. Atmos. Sci.*, 14:433-460.

30 Famiglietti, J. S., and E. F. Wood, 1991, Evapotranspiration and runoff from large  
31 land areas: Land surface hydrology for atmospheric general circulation models. *Surv.*  
32 *Geophys.*, 12: 179-204.

33 Gutowski, W. J., C. J. Vorosmarty, M. Person, Z. Otles, B. Fekete and J. York,  
34 2002: A Coupled Land-Atmosphere Simulation Program (CLASP). *J. Geophys. Res.*, 107  
35 (D16), 4283, 10.1029/2001JD000392

36 Liang, X., E. F. Wood, and D. P. Lettenmaier, 1994, A simple hydrologically-based  
37 model of land surface and energy fluxes for general circulation models. *J. Geophys. Res.*,  
38 99:14 415-14 428.

39 Liang, X., Z. Xie, and M. Huang, 2003, A new parameterization for surface and  
40 groundwater interactions and its impact on water budgets with the variable infiltration  
41 capacity (VIC) land surface model. *J. Geophys. Res.*, 108: 8613, doi:10.1029 /  
42 2002JD003090.

43 Luo, L., and Coauthors, 2003, Effects of frozen soil on soil temperature, spring  
44 infiltration, and runoff: Results from the PILPS 2(d) experiment at Valdai, Russia. *J. of*  
45 *Hydrometeorology*, 4:334-351.

46 Maxwell, R. M., and N. L., Miller, 2005, Development of a Coupled Land  
47 Surface and Groundwater Model. *J. of Hydrometeorology*, 6:233-247.

2 Nash, J. E., and J. V., Sutcliffe, 1970, River flow forecasting through conceptual  
3 models, Part I- A discussion of principles, *J. Hydrology*, 10:282-290.

4 Niu, G.-Y. and Z.-L. Yang, 2006, Assessing a land surface model's improvements  
5 with GRACE estimates *GEOPHYSICAL RESEARCH LETTERS*, VOL. 33, L07401,  
6 doi:10.1029/2005GL025555.

7 Oleson, K. W., and Coauthors, 2004, Technical Description of the Community  
8 Land Model (CLM). NCAR Technical Note/TN-461+STR 173 pp.

9 Robock, A., K. Ya. Vinnikov, G. Srinivasan, J. K. Entin, S. E. Hollinger, N. A.  
10 Speranskaya, S. Liu, and A. Namkhai, 2000, The Global Soil Moisture Data Bank. *Bull.*  
11 *Amer. Meteor. Oc.*, 81:1281-1299.

12 Walko, R. L., and Coauthors, 2000, Coupled atmosphere–biophysics–hydrology  
13 models for environmental modeling. *J. Appl. Meteor.*, 39:931–944.

14 Wood, E. F., D. P. Lettenmaier, and V. G. Zartarian, 1992, A land-surface  
15 hydrology parameterization with subgrid variability for general circulation models. *J.*  
16 *Geophys. Res.*, 97(D3): 2717–2728.

17 Wu, Y.S., C.F. Ahlers, P. Fraser, A. Simmons, and K. Pruess, 1996, Software  
18 Qualification of Selected TOUGH2 Modules. Lawrence Berkeley National Laboratory  
19 Report: LBNL-39490.

20 York, J. P., M. Person, W.J. Gutowski and T. C. Winter, 2002: Putting aquifers  
21 into atmospheric simulation models: An example from the Mill Creek Watershed,  
22 northeastern Kansas. *Adv. Wat. Res.*, 25, 221-238.

23

## 24 **Acknowledgments**

25 The authors would like to thank Keni Zhang and Dan Hawkes for their review of this  
26 paper. Thanks are also due to Reed Maxwell for providing processed observation data  
27 and other help. This work was supported by the U.S. Department of Energy. The support  
28 is provided to Berkeley Lab through the U.S. Department of Energy Contract No. DE-  
29 AC03-76SF00098.

30